Geophysical Research Letters

RESEARCH LETTER
10.1029/2026GL123676

Physical and Biogeochemical Ocean Response to Potential Offshore Wind Development Along the U.S. West Coast

Michael G. Jacox[1,2], Chris Chartrand[3], Ludivine Conte[4], Jerome Fiechter[4], Kaustubha Raghukumar[5], and Grace Chang[5]

[1]Ecosystem Science Division, NOAA Southwest Fisheries Science Center, Monterey, CA, USA, [2]NOAA Physical Sciences Laboratory, Boulder, CO, USA, [3]Sandia National Laboratory, Albuquerque, NM, USA, [4]Ocean Sciences Department, University of California Santa Cruz, Santa Cruz, CA, USA, [5]Integral Consulting Inc., Santa Cruz, CA, USA

Key Points:

- Simulated offshore wind farms alter the spatial distribution of upwelling and associated nitrate supply
- Plankton biomass is altered by circulation anomalies that extend 100s of kilometers from wind farms and modify local nitrate availability
- Regional changes in plankton biomass are ±20% of the mean—small relative to natural variability—and net domain-wide changes are <1%

Supporting Information:

Supporting Information may be found in the online version of this article.

Correspondence to:

M. G. Jacox,
michael.jacox@noaa.gov

Citation:

Jacox, M. G., Chartrand, C., Conte, L., Fiechter, J., Raghukumar, K., & Chang, G. (2026). Physical and biogeochemical ocean response to potential offshore wind development along the U.S. west coast. *Geophysical Research Letters*, *53*, e2026GL123676. https://doi.org/10.1029/2026GL123676

Received 14 APR 2026
Accepted 25 AUG 2026

Abstract Planning for floating offshore wind development along the U.S. west coast has prompted questions about how this new ocean use may impact marine ecosystems. Previous research suggests that offshore wind farms will alter wind dynamics and upwelling in this region, but impacts on biogeochemistry have not yet been explored. Here, we employ a regional atmosphere-ocean-biogoechemistry modeling framework to evaluate the ocean response to simulated wind energy development off Oregon and California. The largest impacts occur during peak upwelling season off central California. Wind stress curl changes at the edges of the wind wake lead to an onshore/offshore dipole of decreased/increased upwelling and associated nitrate supply. Coherent increases and decreases to phytoplankton and zooplankton biomasses occur on larger spatial scales than the wind wake, resulting from circulation changes that alter local nitrate availability. Regional biomass changes are up ±20%, small relative to natural interannual variability, while spatially integrated changes are <1%.

Plain Language Summary The use of offshore wind turbines as a reliable source of renewable energy is expanding globally, and recent years have seen active planning for development along U.S. coastlines. Several regions off California and Oregon are being considered for offshore wind energy, with two of those areas already leased for development. These wind farms have the potential to alter wind patterns that sustain healthy and productive ocean ecosystems, motivating questions about how offshore wind energy may impact the physics and biology of coastal waters. Here, we use numerical models of the atmosphere, ocean, and plankton food web to explore the potential impacts of proposed wind farms. Changes in ocean currents, nutrients, and biological productivity primarily take the form of spatial shifts; some areas experience plankton biomass changes of ±20%, and over the whole domain these regional increases and decreases largely offset each other. Turbine-induced changes occur against the backdrop of strong natural variability, highlighting the importance of using model simulations and observational time series spanning several decades to robustly identify changes. Finally, the mechanism we explore in this paper is one of numerous pathways by which offshore energy installations could drive change, so future research should consider cumulative impacts of development.

1. Introduction

Diverse and sometimes competing ocean uses (e.g., fishing, shipping, offshore energy, marine protected areas) are increasingly complicating marine spatial planning and assessment of potential ecosystem impacts. Development and deployment of offshore wind energy (OWE) is a relatively recent addition to this mélange of human activities, offering one form of renewable energy that can help satisfy a growing energy demand. The science around impacts of OWE (and especially floating wind turbines) on marine ecosystems is similarly in its early days, though myriad possible impacts have been documented (e.g., Farr et al., 2021; Renner, 2025).

In the California Current System (CCS), spanning the west coast of North America, planning for OWE development has been underway in recent years. Two regions off the California coast (Humboldt and Morro Bay) were identified for OWE development, with lease sales occurring in December 2022. Two more areas off Oregon (Coos Bay and Brookings) were initially targeted for OWE development, though at the time of writing any further action has been put on hold. This planned development occurs on the backdrop of a highly dynamic marine ecosystem; the CCS is one of the world's four major eastern boundary upwelling systems, where wind driven

coastal upwelling supports disproportionately high biological productivity and, in turn, human uses including lucrative fisheries and tourism (Bograd et al., 2016; Chavez & Messié, 2009).

Although hundreds of wind farms have been built around the world, most are in relatively shallow water (<30 m) and supported by pilings (Galparsoro et al., 2022). By contrast, the proposed turbines in the CCS will be much larger and in much deeper water (>500 m) than extant OWE structures. While the exact design of the west coast U.S. wind farms has yet to be finalized, they will be placed on floating platforms that are anchored to the sea floor, and will sit in a coastal upwelling system with a relatively narrow continental shelf. There is thus no current analog to the physical and biological impacts of OWE within the CCS.

Given the ecological, social, and economic value of the CCS, it is crucial to understand potential impacts of new OWE development on the environment and the species it supports. Evidence for modification of upwelling in the vicinity of wind farms (e.g., Miles et al., 2021; Raghukumar et al., 2023), together with suggestions from other regions that offshore wind farms can alter ocean circulation, chemistry and productivity (e.g., Christiansen et al., 2022; Daewel et al., 2022; Maar et al., 2026), motivate the current study. Specifically, we seek to quantify potential impacts of proposed offshore wind farms on nutrient availability and plankton biomass off the U.S. west coast.

2. Methods

2.1. Modeling Framework Overview

Wind farm impacts on the atmosphere, ocean, and biogeochemistry are simulated using a suite of models. A regional atmospheric model, the Weather Research and Forecasting model (WRF), is used to simulate the baseline historical atmospheric conditions. A Wind Farm Parameterization within WRF (WRF-WFP; Fitch et al., 2012) simulates the effects of offshore wind turbines, producing perturbed atmospheric forcing. Both the baseline and the perturbed wind forcing are used to drive an ocean-biogeochemical model, the Regional Ocean Modeling System (ROMS; Shchepetkin & McWilliams, 2003; Haidvogel et al., 2008), which is coupled with a version of the North Pacific Ecosystem Model for Understanding Regional Oceanography (NEMURO; Kishi et al., 2007) customized for the CCS (Fiechter et al., 2018, 2020). This overall modeling framework follows from the one used by Raghukumar et al. (2022, 2023), with the addition of ocean biogeochemistry and some modifications to the model configuration, noted below. Simulations presented here were performed over a 24-year period from 1996 to 2019.

2.2. Atmospheric Model

The WRF domain covers the U.S. west coast and extends ∼1,000 km offshore, spanning 29.5–48.5°N and 136-110°W. The full domain has 1/30° (∼3 km) resolution, whereas Raghukumar et al. (2023) used a 1/30° nest in a 1/10° outer domain. Boundary and initial conditions were derived from the European Centre for Medium-Range Weather Forecasts (ECMWF) atmospheric reanalysis version 5 (ERA5; Hersbach et al., 2020). In Raghukumar et al. (2023), WRF simulations were run 24 hr at a time, saving snapshots every 3 hr. Here, WRF simulations were run 1 year at a time. For each year, the simulation was started December 1st of the prior year, such that the total run was 13 months long and the first month was discarded to avoid spin-up effects. Output was saved as 3-hr averages to force the ocean model.

In WRF-WFP, wind turbines are parameterized as a momentum sink and a turbulence source. While the individual turbines are sub grid scale, the magnitude of the source and sink terms is calculated based on specifications including hub height, rotor diameter, and thrust coefficient (Lee & Lundquist, 2017). The model also accounts for turbine-turbine and wake-turbine interactions to provide a realistic simulation of the net wind farm impact on the wind field (Churchfield et al., 2012). While this parameterization was developed for fixed-bottom turbines, we are unaware of evidence that it should be altered to account for potential wake perturbations from platform motion of floating turbines. Nonetheless, we note this as an open research question.

Turbine specifications for 15 and 20 MW turbines, larger than the 10 MW turbines used in Raghukumar et al. (2023), are from Gaertner et al. (2020). Hub heights are 150 and 180 m for the 15 and 20 MW turbines, respectively, while rotor diameters are 240 and 310 m. Simulations assume full buildout of four areas identified for potential OWE development off Oregon and California (Figure 1). Turbine spacing is 10 and 4 rotor diameters, respectively, in the directions parallel and perpendicular to the prevailing wind (Wallach et al., 2021).

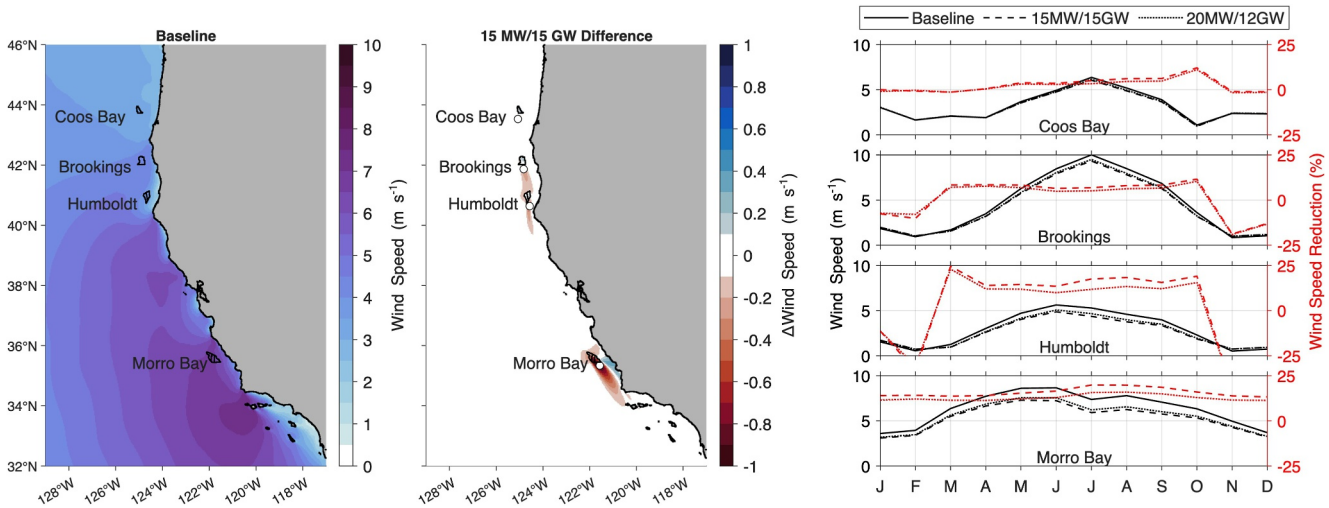

Figure 1. Surface wind modifications by simulated offshore wind farms. (left) Long-term mean wind speed from the baseline run, (middle) mean wind speed change induced by simulated buildouts of four wind energy areas or areas of interest with 15 MW turbines (15 GW total capacity), and (right) climatological wind speed (black lines) for each simulation at points in the wind wakes of each simulated wind farm (white dots in middle panel), with % changes (red lines) for each wind farm simulation. Simulated wind farms are outlined in the left and middle panels.

The larger 20 MW turbines require wider spacing, resulting in fewer total turbines (131, 55, 135, and 274 turbines for Brookings, Coos Bay, Humboldt, and Morro Bay, respectively, vs. 15 MW turbine counts of 215, 90, 214, and 453). Consequently, the 20 MW turbine configuration generates less total power than the 15 MW configuration (11,900 MW vs. 14,580 MW) across the four simulated wind farms. Since the 15 and 20 MW turbine configurations have different total capacities, we refer to them hereafter by both turbine size and total capacity (i.e., 15 MW/15 GW and 20 MW/12 GW).

2.3. Ocean-Biogeochemical Model

The coupled ocean-biogeochemical model domain spans 30–48°N and 134–115.5°W at 1/30° horizontal resolution (aligned with the WRF grid), with 42 terrain-following vertical levels. The biogeochemical model includes 11 prognostic variables; of particular interest here are nitrate concentration as well as concentrations of two phytoplankton size classes (nanophytoplankton and diatoms) and three zooplankton size classes (micro-, meso-, and predatory zooplankton). Surface forcing for ROMS was obtained from the WRF runs described above, and ROMS was run in a continuous 24-year simulation. For the lateral ocean boundary conditions, physical fields were generated from the Global Ocean Reanalysis and Simulations (GLORYS) global 1/12° ocean reanalysis (Lellouche et al., 2021), while biogeochemical fields were obtained from the GLORYS Global Ocean Biogeochemical Hindcast (https://doi.org/10.48670/moi-0001). Model runs were initialized with the GLORYS physical and biogeochemical fields from 1 January 1994 and the first two years of the simulation (1994–95) were discarded to remove spinup effects. Past evaluations of this CCS model configuration illustrate its fidelity to nature; surface chlorophyll concentrations faithfully reproduce the observed alongshore structure in terms of both mean and variance during the upwelling season (Fiechter et al., 2018; their Figure 2), while modeled krill concentrations exhibit hot spots in the same locations as observations and capture approximately half of the observed variance (Fiechter et al., 2020). This configuration has been used in wide-ranging studies addressing fundamental physical and biogeochemical processes in the CCS, ecological responses of species from phytoplankton to higher trophic level predators, and interactions of the marine environment with human activities (e.g., Cheresh et al., 2023; Fiechter et al., 2020; Raghukumar et al., 2023; Vasbinder et al., 2024).

A suite of four 24-year simulations was run to evaluate the potential impacts of wind farms and the robustness of those impacts in the presence of natural variability: (1) a baseline case (no turbines), (2–3) turbine cases for two turbine sizes (15 MW/15 GW and 20 MW/12 GW), and (4) an additional run using the 15 MW/15 GW forcing but with the initial condition taken from the end of the original 15 MW/15 GW simulation (simulation 2). This final simulation was included to document the sensitivity of our results to the initial ocean condition (i.e., due to internal ocean variability).

2.4. Analyses

Our analyses focus on changes to atmospheric and oceanic fields induced by the addition of offshore wind farms. Key properties include surface wind stress, upwelling magnitude as measured by the Coastal Upwelling Transport Index (CUTI), upwelled nitrate supply as measured by the Biologically Effective Upwelling Transport Index (BEUTI), sea surface height (SSH), subsurface nitrate concentration, and upper ocean phytoplankton and zooplankton concentrations. All variables are obtained directly from the model output. CUTI is the sum of Ekman and geostrophic transports integrated around the area of interest, calculated based on surface wind stress, SSH, and mixed layer depth (Jacox et al., 2018). BEUTI is the product of CUTI and nitrate concentration at the base of the mixed layer. In contrast to Jacox et al. (2018), who used physical proxies to estimate nitrate concentration, here we use the nitrate concentration from the biogeochemical model.

Considering that the signal-to-noise ratio for some wind-farm related impacts is relatively weak (discussed later), our analysis focuses on monthly to seasonal timescales and long-term means. Similarly, we primarily present results averaged across the 15 MW/15 GW and 20 MW/12 GW wind turbine configurations in order to highlight changes that are robust to the details of development, though differences between configurations are also shown. We test for significance of physical and biogeochemical changes with paired *t*-tests based on seasonal mean values ($N = 24$). Effective sample size (N_{eff}) is calculated based on the lag-1 autocorrelation (r_1) according to $N_{eff} = N^*(1 - r_1)/(1 + r_1)$. Finally, when reporting spatially integrated changes in physical and biogeochemical variables, we use an integration area covering 116–126°W and 32–44°N.

3. Results

3.1. Wind

The extraction of energy by offshore wind farms is evident in the surface wind speed deficits, or wind wakes, in their lees. In annual mean wind speeds, wakes extend ∼100–200 km downstream of each wind farm with the exception of Coos Bay, for which small wind reductions occur only in the spring and summer months (Figure 1). Wind speed reductions near Morro Bay occur year-round, consistent with persistent upwelling-favorable winds there. Surface wind deficits in the region are ∼15%–20% of the long-term mean, comparable to reductions from North Sea wind farms (Akhtar et al., 2024), with the magnitude of reductions reaching ∼1.5 m s^{-1} in peak upwelling season. The other wind areas see more seasonality in both wind speed and wind speed deficits; Humboldt's relative changes are similar to Morro Bay (15%–25%), though they are smaller in absolute terms, while the changes for Oregon areas are smaller in both absolute and relative terms (∼0%–5% for Coos Bay, ∼5%–10% for Brookings). Wind speed reductions in the 20 MW/12 GW and 15 MW/15 GW simulations are qualitatively similar, though slightly less pronounced for 20 MW/12 GW.

3.2. Upwelling

Downstream of each wind farm, reduced surface wind speeds induce negative (positive) wind stress curl changes on the inshore (offshore) side of the wind wake, which in turn drive negative (positive) upwelling anomalies (Figure 2; Floeter et al., 2022; Raghukumar et al., 2023). Consistent with changes in the winds themselves, the strongest upwelling impacts are seen off Morro Bay, with qualitatively similar but lower magnitude impacts off Humboldt and Oregon. The strength of upwelling is proportional to wind stress, and thus proportional to the square of the wind speed, so changes in upwelling are amplified relative to changes in wind speed. Since these changes occur in an area with relatively weak mean upwelling (i.e., offshore of the narrow band of intense mean coastal upwelling), they shift the spatial upwelling pattern well outside of its natural bounds (in agreement with Raghukumar et al., 2023). Nitrate supplied by upwelling (i.e., BEUTI) also exhibits decreases on the inshore side of wind wakes and increases on their offshore sides (Figure 2); this pattern is driven primarily by changes in upwelling strength, not by changes in the nitrate content of upwelled water. The total coast-wide upwelling, integrated across areas of increase and decrease, is effectively unchanged (0.2% for CUTI, 0.0% for BEUTI).

3.3. Circulation Changes and Nitrate

Beyond the modifications to upwelling in the immediate vicinity of the wind wake, the simulations with wind farms also exhibit near-surface circulation changes with a larger footprint during the upwelling season. Specifically, offshore of the Morro Bay wind farm there is a depression in SSH extending several hundred kilometers

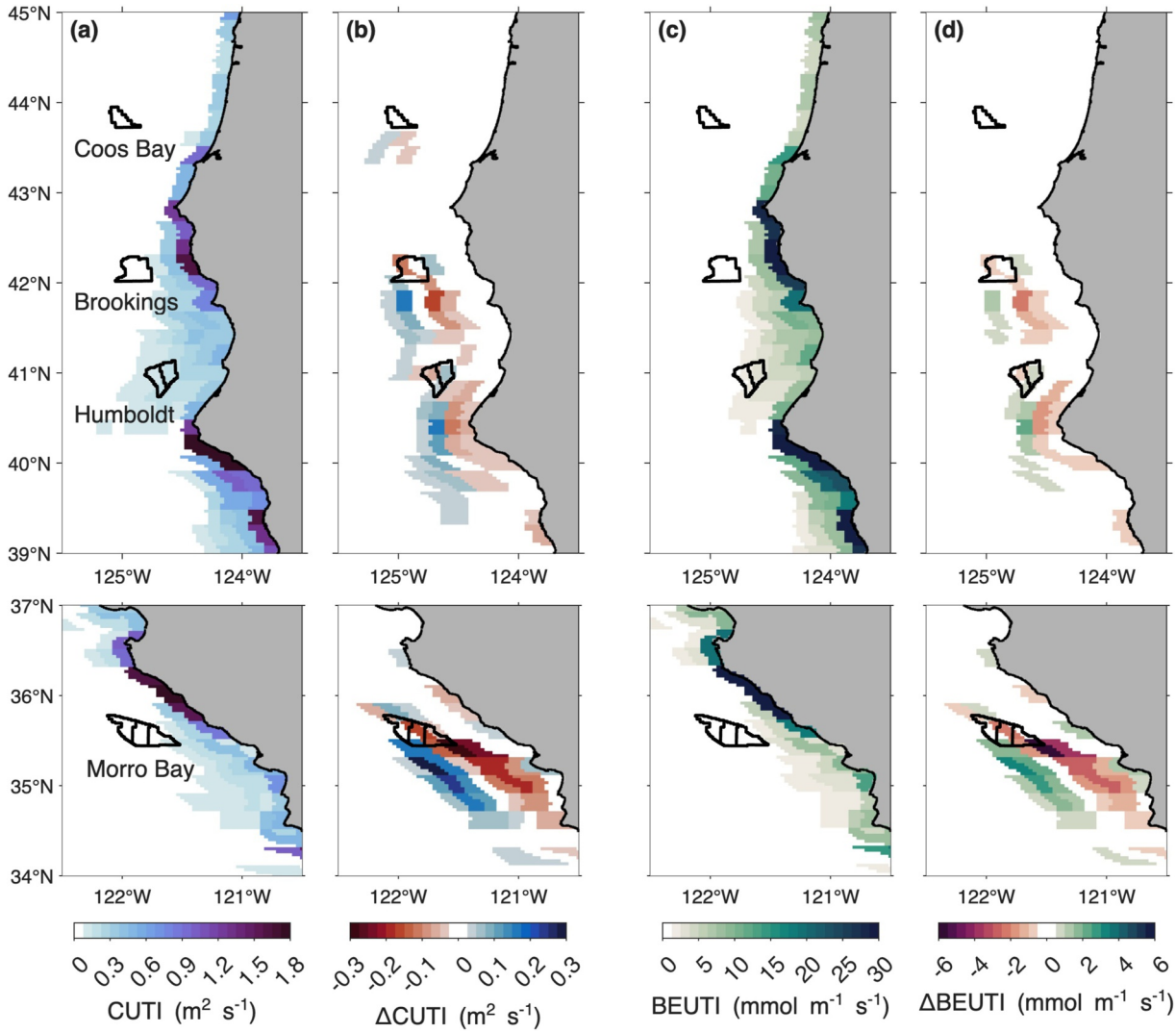

Figure 2. Upwelling modification by simulated offshore wind farms. Mean (a) upwelling magnitude, CUTI, and (c) nitrate supply, BEUTI, off Oregon and Northern California (top) and central California (bottom) for the baseline case with no offshore wind farms. (b, d) Changes induced by simulated offshore wind farms averaged across the 15 MW/15 GW and 20 MW/12 GW turbine configurations for April–July, the peak upwelling season in the Morro Bay region.

offshore, with a corresponding region of elevated SSH to the south, associated with an offshore displacement of the meandering coastal upwelling jet (Figures 3 and 4). Previous studies have shown this response to an inshore injection of positive wind stress curl, where isopycnals tilt upward in the offshore region, southward velocities intensify due to the associated pressure gradient, and cyclonic/anticyclonic circulation anomalies can extend hundreds of kilometers away (Aguirre et al., 2012; Castelao & Barth, 2006, 2007). In the region of SSH depression and cyclonic circulation anomalies, isopycnals and nitrate surfaces uplift, while the opposite occurs in the region of anticyclonic circulation anomalies to the south. This general pattern is consistent across the three different wind farm simulations (Figure S1 in Supporting Information S1).

3.4. Plankton

The most prominent changes in phytoplankton and zooplankton biomass are coincident with the areas of modified SSH and nitrate concentrations described above (Figure 5). In the region offshore of the Morro Bay wind wake, where simulated nitrate isolines shoal and surface layer nitrate availability is enhanced, phytoplankton and zooplankton biomass during the upwelling season increases by ~20%. Decreases in plankton biomass of similar magnitude are evident in the area of reduced nitrate concentrations to the south. As is the case for upwelling, the

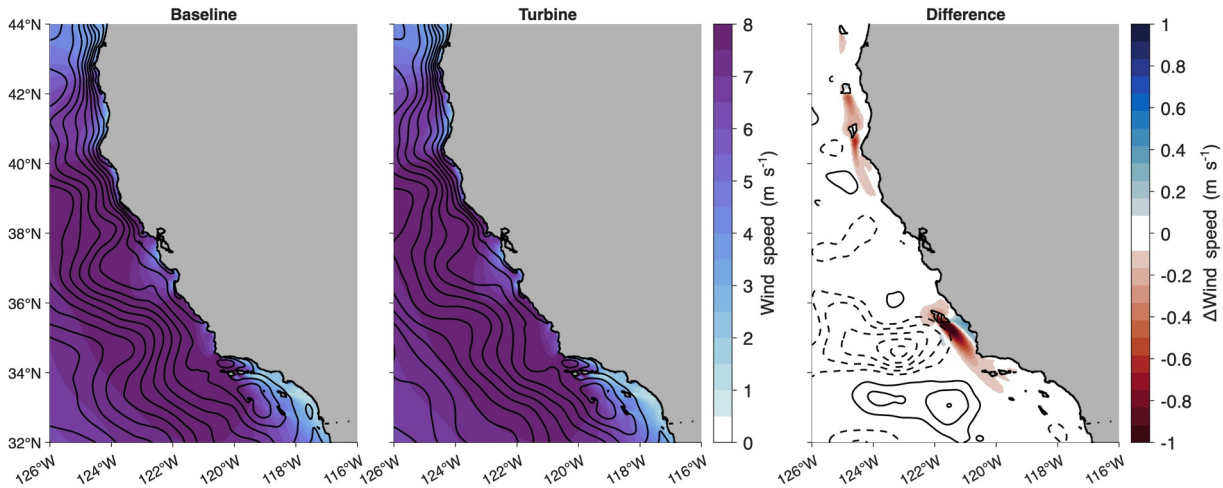

Figure 3. Wind speed (color) and sea surface height (contours) for (left) the baseline case, (middle) the simulation with turbines, and (right) the difference between the two. SSH contours are in 2 cm increments. SSH difference contours are in 1 cm increments, with dashes indicating negative values. Panels show April–July averages, and turbine fields are averaged across the 15 MW/15 GW and 20 MW/12 GW simulations.

biomass increases and decreases largely cancel, such that domain-integrated biomass changes are just 0.6% and 0.2% for phytoplankton and zooplankton, respectively. The regional changes in biomass are accompanied by changes in the plankton community composition. Areas with increased biomass also exhibit shifts toward larger plankton groups, while the opposite is true in areas of decreased biomass (Figure S2 in Supporting Information S1), consistent with the understanding that smaller plankton are favored in low nutrient conditions while larger plankton are favored in nutrient-replete conditions (e.g., Falkowski & Oliver, 2007; Marañón, 2015). While the tight spatial overlap of plankton changes with those of SSH and nitrate suggests causality, there could also be an influence of the altered upwelling near shore, through advection coupled with lags in the plankton response (e.g., increased upwelled nitrate on the offshore edge of the wind wake is carried offshore by the mean circulation and stimulates increased productivity farther offshore). Nonetheless, changes are still relatively small in the

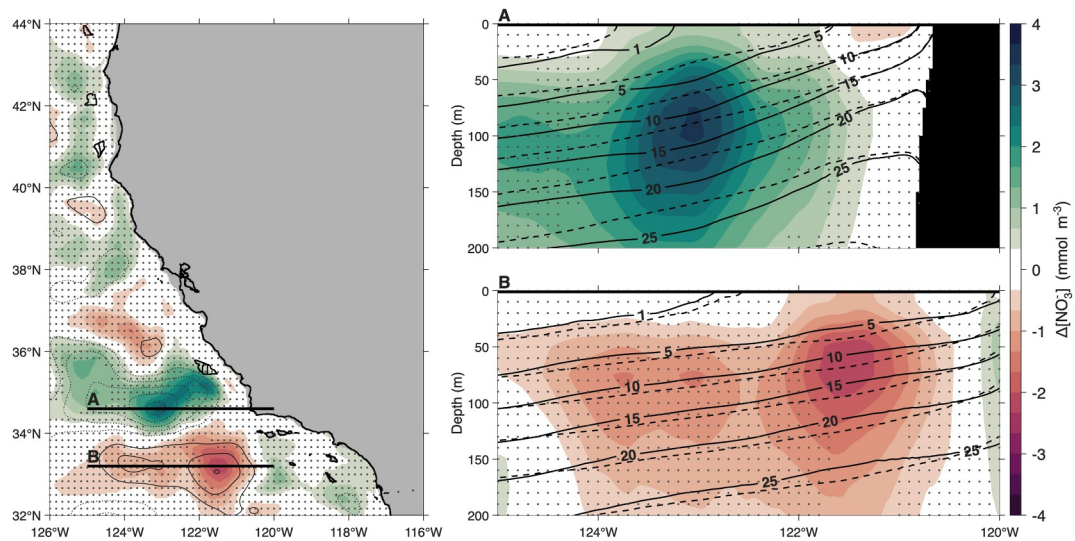

Figure 4. (left) SSH differences induced by simulated offshore wind farms (contours) overlaid on changes in nitrate concentration at 50 m depth (color). SSH difference contours are as in Figure 3. (right) Nitrate changes (color) and contours for the baseline case (solid lines) and turbine case (dashed lines) along two zonal transects where greatest SSH and nitrate changes occur (black lines on map). Stippling indicates nitrate changes that are not significant ($p > 0.05$). For clarity, stippling is subsampled at every 5th grid point (1/6°) in the map at left, and at 0.1° longitude/10 m depth in the sections at right. Significance of SSH changes is very similar to that of nitrate changes (Figure S4 in Supporting Information S1). Panels show April–July averages, and turbine fields are averaged across the 15 MW/15 GW and 20 MW/12 GW simulations.

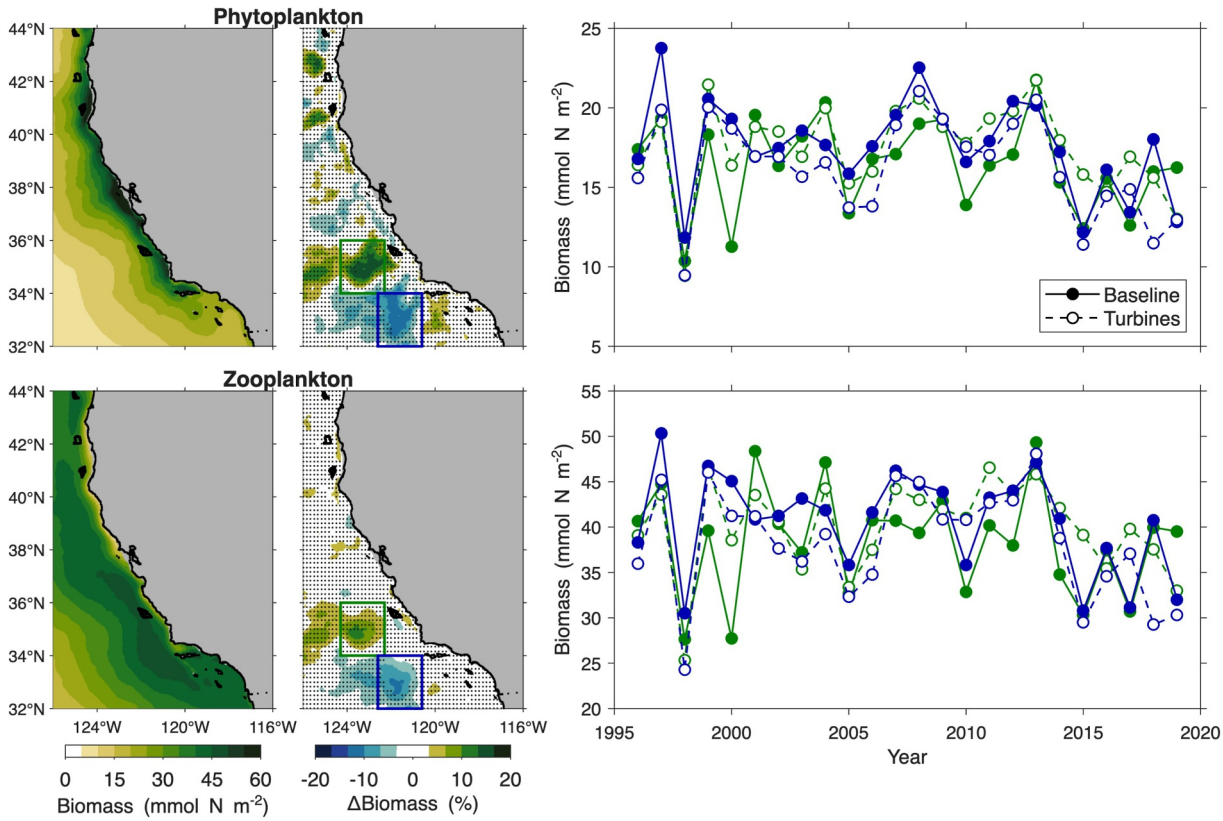

Figure 5. Plankton changes associated with simulated wind farms. For (top) phytoplankton and (bottom) zooplankton, (left) mean biomass integrated over the upper 50 m for baseline case and (middle) changes in simulations with wind farms. Maps show April–July averages, and turbine fields are averaged across the 15 MW/15 GW and 20 MW/12 GW simulations. Stippling indicates differences that are not statistically significant ($p > 0.05$). For clarity, stippling is subsampled at every 5th grid point (1/6°). (right) Time series of (top) phytoplankton and (bottom) zooplankton averaged over regions of increased (green) and decreased (blue) biomass. Time series data are annual means for April–July.

context of interannual variability. When looking at the time series from the area of increased mean plankton biomass, those increases are not consistent year-to-year, and the same is true for the area of decreased biomass (Figure 5).

Changes in plankton biomass throughout the rest of the domain are more subtle and generally less robust across wind farm simulations, suggesting that signals are small relative to noise. Outside of the upwelling season, similar patterns appear, but are much reduced in magnitude (Figure S3 in Supporting Information S1). One small but consistent pattern during the upwelling season is a dipole of increased/decreased zooplankton biomass along the Morro Bay wind wake. Interestingly, these changes in zooplankton biomass are of opposite sign to those in the nitrate flux (BEUTI), with increased (decreased) biomass on the inshore (offshore) edge of the wind wake. This somewhat counterintuitive finding may reflect an increase in biomass nearshore associated with weaker Ekman transport and reduced offshore advection, an effect that can be much more pronounced for zooplankton than phytoplankton (e.g., Botsford et al., 2006).

4. Discussion

Using an atmosphere-ocean-biogeochemistry modeling framework, we evaluated potential changes in the physical and biogeochemical mean state of the CCS as a result of offshore wind energy development. The most robust changes occur during the upwelling season in response to the pronounced wind wake downstream of the Morro Bay wind farm, and include (a) increased (decreased) upwelling and nitrate supply on the offshore (inshore) edge of the wind wake, (b) depressed SSH and uplifted nitrate isolines associated with a cyclonic circulation anomaly offshore of the wind wake, with a corresponding opposite pattern to the south, and (c) positive and negative phytoplankton and zooplankton biomass changes of ~20% overlapping with these

circulation anomalies, coupled with shifts in plankton community composition. While the fine-scale details of upwelling season changes differ between the various wind farm simulations (i.e.., 15 MW/15 GW vs. 20 MW/12 GW; 15 MW/15 GW runs with different initial conditions), the qualitative patterns described here appear robust to changing wind farm configurations (Figure S1 in Supporting Information S1). Changes in the vicinity of the more northern wind farms and outside of the upwelling season were typically smaller and/or noisier.

As a dynamic Eastern Boundary Upwelling System in the North Pacific, the CCS is highly variable on intra-seasonal to interannual timescales. Interannual and decadal variability can make detection of mean state changes and trends challenging (e.g., Henson et al., 2017). For example, even over multi-decadal periods, cooling has prevailed despite a longer-term warming trend (Seo et al., 2012). Similar signal-to-noise limitations apply to detection of changes induced by offshore wind farm development. In our numerical experiments, we find that individual years can exhibit apparent changes that are in opposition to the expected long-term mean changes, and multiple decades of simulation are required to elucidate change. Even then, mean changes are smaller than natural interannual variability (e.g., Figure 5) and can quantitatively change based on the initial state of the ocean (Figure S1 in Supporting Information S1; 15 MW/15 GW cf. 15 MW/15 GW rerun). Thus, we reiterate the importance of long model runs and observational time series to robustly quantify human-induced changes relative to natural variability (Kojima et al., 2024), as the latter can dominate even on multi-year timescales. Notably, lines 73 and 83 of the long-running California Cooperative Oceanic Fisheries Investigations (CalCOFI) pass through the areas of simulated plankton increase and decrease, respectively.

Given the computational expense of running the atmospheric and ocean-biogeochemistry models at high spatial resolution, we were pragmatic in our choice of simulations. For instance, our analysis could be expanded to encompass changes in wind energy areas, build-out scenarios, and turbine parameters, potentially identifying design choices that minimize impacts (Akhtar et al., 2024). Ocean-atmosphere feedbacks in response to changes induced by wind farms, including eddy-wind interactions, could also be explored with two-way air-sea coupling (Seo et al., 2016, 2025). Furthermore, modification of the surface wind field, and consequently ocean circulation and biogeochemistry, is just one of many mechanisms by which offshore wind development may impact ecosystem functions. Others include habitat alteration by in-water structures and cables, marine species' responses to electromagnetic fields from power cables, and underwater noise (Farr et al., 2021), as well as interactions with other ocean uses such as fisheries (Warlick et al., 2025). Hence, our results should be taken as one piece of the larger puzzle of understanding potential OWE impacts on marine ecosystems.

Conflict of Interest

The authors declare no conflicts of interest relevant to this study.

Availability Statement

Data and code to reproduce figures are available in Jacox (2026).

Acknowledgments
Funding for initial development of the atmosphere-ocean modeling framework was provided by the California Energy Commission Electric Program Investment Charge Program (EPC-19-009) and the California Ocean Protection Council (C0210404). Conceptual turbine layouts were provided by the Schatz Energy Research Center. We thank Andrew Thompson, Jack Barth, and an anonymous referee for comments on an earlier version of the manuscript.

References

Aguirre, C., Pizarro, Ó., Strub, P. T., Garreaud, R., & Barth, J. A. (2012). Seasonal dynamics of the near-surface alongshore flow off central Chile. *Journal of Geophysical Research*, *117*(C1). https://doi.org/10.1029/2011jc007379

Akhtar, N., Geyer, B., & Schrum, C. (2024). Larger wind turbines as a solution to reduce environmental impacts. *Scientific Reports*, *14*(1), 6608. https://doi.org/10.1038/s41598-024-56731-w

Bograd, S. J., Hazen, E. L., Maxwell, S., Leising, A. W., Bailey, H., & Brodeur, R. (2016). Offshore ecosystems. In H. Mooney & E. Zavaleta (Eds.), *Ecosystems of California—A source book* (pp. 287–309). University of California Press.

Botsford, L. W., Lawrence, C. A., Dever, E. P., Hastings, A., & Largier, J. (2006). Effects of variable winds on biological productivity on continental shelves in coastal upwelling systems. *Deep Sea Research Part II: Topical Studies in Oceanography*, *53*(25–26), 3116–3140. https://doi.org/10.1016/j.dsr2.2006.07.011

Castelao, R. M., & Barth, J. A. (2006). The relative importance of wind strength and along-shelf bathymetric variations on the separation of a coastal upwelling jet. *Journal of Physical Oceanography*, *36*(3), 412–425. https://doi.org/10.1175/jpo2867.1

Castelao, R. M., & Barth, J. A. (2007). The role of wind stress curl in jet separation at a cape. *Journal of Physical Oceanography*, *37*(11), 2652–2671. https://doi.org/10.1175/2007jpo3679.1

Chavez, F. P., & Messié, M. (2009). A comparison of eastern boundary upwelling ecosystems. *Progress in Oceanography*, *83*(1–4), 80–96. https://doi.org/10.1016/j.pocean.2009.07.032

Cheresh, J., Kroeker, K. J., & Fiechter, J. (2023). Upwelling intensity and source water properties drive high interannual variability of corrosive events in the California current. *Scientific Reports*, *13*(1), 13013. https://doi.org/10.1038/s41598-023-39691-5

Christiansen, N., Daewel, U., Djath, B., & Schrum, C. (2022). Emergence of large-scale hydrodynamic structures due to atmospheric offshore wind farm wakes. *Frontiers in Marine Science*, *9*, 818501. https://doi.org/10.3389/fmars.2022.818501

Churchfield, M. J., Lee, S., Michalakes, J., & Moriarty, P. J. (2012). A numerical study of the effects of atmospheric and wake turbulence on wind turbine dynamics. *Journal of Turbulence*, *13*(13), N14. https://doi.org/10.1080/14685248.2012.668191

Daewel, U., Akhtar, N., Christiansen, N., & Schrum, C. (2022). Offshore wind farms are projected to impact primary production and bottom water deoxygenation in the North Sea. *Communications Earth & Environment*, *3*(1), 292. https://doi.org/10.1038/s43247-022-00625-0

Falkowski, P. G., & Oliver, M. J. (2007). Mix and match: How climate selects phytoplankton. *Nature Reviews Microbiology*, *5*(10), 813–819. https://doi.org/10.1038/nrmicro1751

Farr, H., Ruttenberg, B., Walter, R. K., Wang, Y. H., & White, C. (2021). Potential environmental effects of deepwater floating offshore wind energy facilities. *Ocean & Coastal Management*, *207*, 105611. https://doi.org/10.1016/j.ocecoaman.2021.105611

Fiechter, J., Edwards, C. A., & Moore, A. M. (2018). Wind, circulation, and topographic effects on alongshore phytoplankton variability in the California current. *Geophysical Research Letters*, *45*(7), 3238–3245. https://doi.org/10.1002/2017gl076839

Fiechter, J., Santora, J. A., Chavez, F., Northcott, D., & Messié, M. (2020). Krill hotspot formation and phenology in the California current ecosystem. *Geophysical Research Letters*, *47*(13), e2020GL088039. https://doi.org/10.1029/2020gl088039

Fitch, A. C., Olson, J. B., Lundquist, J. K., Dudhia, J., Gupta, A. K., Michalakes, J., & Barstad, I. (2012). Local and mesoscale impacts of wind farms as parameterized in a mesoscale NWP model. *Monthly Weather Review*, *140*(9), 3017–3038. https://doi.org/10.1175/mwr-d-11-00352.1

Floeter, J., Pohlmann, T., Harmer, A., & Möllmann, C. (2022). Chasing the offshore wind farm wind-wake-induced upwelling/downwelling dipole. *Frontiers in Marine Science*, *9*, 884943. https://doi.org/10.3389/fmars.2022.884943

Gaertner, E., Rinker, J., Sethuraman, L., Zahle, F., Anderson, B., Barter, G. E., et al. (2020). *IEA wind TCP task 37: Definition of the IEA 15-megawatt offshore reference wind turbine (no. NREL/TP-5000-75698)*. National Renewable Energy Lab.(NREL).

Galparsoro, I., Menchaca, I., Garmendia, J. M., Borja, Á., Maldonado, A. D., Iglesias, G., & Bald, J. (2022). Reviewing the ecological impacts of offshore wind farms. *npj Ocean Sustainability*, *1*(1), 1. https://doi.org/10.1038/s44183-022-00003-5

Haidvogel, D. B., Arango, H., Budgell, W. P., Cornuelle, B. D., Curchitser, E., Di Lorenzo, E., et al. (2008). Ocean forecasting in terrain-following coordinates: Formulation and skill assessment of the regional ocean modeling system. *Journal of Computational Physics*, *227*(7), 3595–3624. https://doi.org/10.1016/j.jcp.2007.06.016

Henson, S. A., Beaulieu, C., Ilyina, T., John, J. G., Long, M., Séférian, R., et al. (2017). Rapid emergence of climate change in environmental drivers of marine ecosystems. *Nature Communications*, *8*(1), 14682. https://doi.org/10.1038/ncomms14682

Hersbach, H., Bell, B., Berrisford, P., Hirahara, S., Horányi, A., Muñoz-Sabater, J., et al. (2020). The ERA5 global reanalysis. *Quarterly Journal of the Royal Meteorological Society*, *146*(730), 1999–2049. https://doi.org/10.1002/qj.3803

Jacox, M. G. (2026). Data files for Jacox et al., Physical and biogeochemical ocean response to potential offshore wind development along the U.S. west coast. *Zenodo*. [Dataset]. https://doi.org/10.5281/zenodo.22049184

Jacox, M. G., Edwards, C. A., Hazen, E. L., & Bograd, S. J. (2018). Coastal upwelling revisited: Ekman, Bakun, and improved upwelling indices for the US West Coast. *Journal of Geophysical Research: Oceans*, *123*(10), 7332–7350. https://doi.org/10.1029/2018jc014187

Kishi, M. J., Kashiwai, M., Ware, D. M., Megrey, B. A., Eslinger, D. L., Werner, F. E., et al. (2007). NEMURO—A lower trophic level model for the North Pacific marine ecosystem. *Ecological Modelling*, *202*(1–2), 12–25. https://doi.org/10.1016/j.ecolmodel.2006.08.021

Kojima, A., Kilpatrick, T., Jacox, M., Tourjé-Maldonado, J., Valdez, B., & Cabrera, J., (2024). *Observational and modeling approaches for assessing impacts of offshore wind development on California current upwelling: Workshop summary – march 4, 2024*. Workshop report prepared by Kearns & West for the U.S. Department of the Interior, Bureau of Ocean Energy Management, Pacific Regional Office, Camarillo, CA. (p. 24). Report No.: OCS Study BOEM 2024-049. Contract No.: 140D0423D0077

Lee, J. C., & Lundquist, J. K. (2017). Evaluation of the wind farm parameterization in the weather research and forecasting model (version 3.8. 1) with meteorological and turbine power data. *Geoscientific Model Development*, *10*(11), 4229–4244. https://doi.org/10.5194/gmd-10-4229-2017

Lellouche, J.-M., Greiner, E., Bourdallé Badie, R., Garric, G., Melet, A., Drevillon, M., et al. (2021). The copernicus global 1/12∘ Oceanic and sea ice GLORYS12 reanalysis. *Frontiers in Earth Science*, *9*. https://doi.org/10.3389/feart.2021.698876

Maar, M., Schourup-Kristensen, V., Mohn, C., Ishimwe, A. P., Friis Møller, E., Clubley, C. H., et al. (2026). Offshore wind farms reshape ocean stratification and productivity differently in the North Sea and the Baltic Sea. *Npj Ocean Sustainability*, *5*(38), 38. https://doi.org/10.1038/s44183-026-00202-4

Marañón, E. (2015). Cell size as a key determinant of phytoplankton metabolism and community structure. *Annual Review of Marine Science*, *7*(1), 241–264. https://doi.org/10.1146/annurev-marine-010814-015955

Miles, T., Murphy, S., Kohut, J., Borsetti, S., & Munroe, D. (2021). Offshore wind energy and the mid-Atlantic cold pool: A review of potential interactions. *Marine Technology Society Journal*, *55*(4), 72–87. https://doi.org/10.4031/mtsj.55.4.8

Raghukumar, K., Chartrand, C., Chang, G., Cheung, L., & Roberts, J. (2022). Effect of floating offshore wind turbines on atmospheric circulation in California. *Frontiers in Energy Research*, *10*, 863995. https://doi.org/10.3389/fenrg.2022.863995

Raghukumar, K., Nelson, T., Jacox, M., Chartrand, C., Fiechter, J., Chang, G., et al. (2023). Projected cross-shore changes in upwelling induced by offshore wind farm development along the California coast. *Communications Earth & Environment*, *4*(1), 116. https://doi.org/10.1038/s43247-023-00780-y

Renner, A. H. H. (2025). Current knowledge and key gaps in understanding of offshore wind farm impacts on the physical marine environment. *ICES Journal of Marine Science*, *82*(12), fsaf235. https://doi.org/10.1093/icesjms/fsaf235

Seo, H., Brink, K. H., Dorman, C. E., Koracin, D., & Edwards, C. A. (2012). What determines the spatial pattern in summer upwelling trends on the US West Coast? *Journal of Geophysical Research*, *117*(C8). https://doi.org/10.1029/2012jc008016

Seo, H., Miller, A. J., & Norris, J. R. (2016). Eddy-wind interaction in the California current system: Dynamics and impacts. *Journal of Physical Oceanography*, *46*(2), 439–459. https://doi.org/10.1175/jpo-d-15-0086.1

Seo, H., Sauvage, C., Renkl, C., Lundquist, J. K., & Kirincich, A. (2025). Sea surface warming and ocean-to-atmosphere feedback driven by large-scale offshore wind farms under seasonally stratified conditions. *Science Advances*, *11*(45), eadw7603. https://doi.org/10.1126/sciadv.adw7603

Shchepetkin, A. F., & McWilliams, J. C. (2003). A method for computing horizontal pressure-gradient force in an oceanic model with a nonaligned vertical coordinate. *Journal of Geophysical Research*, *108*(C3). https://doi.org/10.1029/2001jc001047

Vasbinder, K., Fiechter, J., Santora, J. A., Anderson, J. J., Mantua, N., Lindley, S. T., et al. (2024). Size-selective predation effects on juvenile Chinook salmon cohort survival off Central California evaluated with an individual-based model. *Fisheries Oceanography*, *33*(1), e12654. https://doi.org/10.1111/fog.12654

Wallach, E., Carman, J., Alva, Z., Chamberlin, C., & Jacobson, A. (2021). EPC-19-011: Seabird 3D distribution and relative vulnerability to California offshore wind development, task 4: Offshore wind power generation report.

Warlick, A. J., Liu, O. R., Layton, J., Harvey, C. J., Samhouri, J. F., Hazen, E. L., & Andrews, K. S. (2025). A framework to evaluate dynamic social and ecological interactions between offshore wind energy development and commercial fisheries in a changing climate: A US West Coast perspective. *PLOS Climate*, *4*(5), e0000526. https://doi.org/10.1371/journal.pclm.0000526